HHS Public Access

Author manuscript

Cancer Discov. Author manuscript; available in PMC 2018 January 01.

Published in final edited form as:

Cancer Discov. 2017 January ; 7(1): 72–85. doi:10.1158/2159-8290.CD-16-0502.

Tumor Cell-Independent Estrogen Signaling Drives Disease Progression Through Mobilization of Myeloid-Derived Suppressor Cells

Nikolaos Svoronos[1], **Alfredo Perales-Puchalt**[1], **Michael J. Allegrezza**[1], **Melanie R. Rutkowski**[1], **Kyle K. Payne**[1], **Amelia J. Tesone**[1], **Jenny M. Nguyen**[1], **Tyler J. Curiel**[2,3,4], **Mark G. Cadungog**[5], **Sunil Singhal**[6], **Evgeniy B. Eruslanov**[6], **Paul Zhang**[7], **Julia Tchou**[8], **Rugang Zhang**[9], and **Jose R. Conejo-Garcia**[1,#]

[1]Tumor Microenvironment and Metastasis Program, The Wistar Institute, Philadelphia, PA 19104, USA

[2]The Graduate School of Biomedical Sciences, University of Texas Health Science Center, San Antonio, TX 78229

[3]Department of Medicine, University of Texas Health Science Center, San Antonio, TX 78229

[4]Cancer Therapy & Research Center, University of Texas Health Science Center, San Antonio, TX 78229

[5]Helen F. Graham Cancer Center, Christiana Care Health System, 4701 Ogletown-Stanton Road, Newark, DE 19713, USA

[6]Divisions of Thoracic Surgery, University of Pennsylvania, Philadelphia, PA 19104

[7]Department of Pathology and Laboratory Medicine, University of Pennsylvania, Philadelphia, PA 19104

[8]Endocrine and Oncologic Surgery, Department of Surgery, University of Pennsylvania, Philadelphia, PA 19104

[9]Gene Expression and Regulation Program, The Wistar Institute, Philadelphia, PA 19104, USA

Abstract

The role of estrogens in anti-tumor immunity remains poorly understood. Here we show that estrogen signaling accelerates the progression of different estrogen insensitive tumor models by contributing to deregulated myelopoiesis by both driving the mobilization of myeloid-derived suppressor cells (MDSCs) and enhancing their intrinsic immunosuppressive activity *in vivo*. Differences in tumor growth are dependent on blunted anti-tumor immunity and, correspondingly, disappear in immunodeficient hosts and upon MDSC depletion. Mechanistically, estrogen receptor alpha activates the STAT3 pathway in human and mouse bone marrow myeloid precursors by enhancing JAK2 and SRC activity. Therefore, estrogen signaling is a crucial mechanism

[#]Correspondence: Jose R Conejo-Garcia, MD, PhD, The Wistar Institute, 3601 Spruce St, Philadelphia, PA 19104, Phone: (215) 495-6825, Fax: (215) 898-0847, jrconejo@Wistar.org.

COI: The authors declare no conflict of interest

underlying pathological myelopoiesis in cancer. Our work suggests that new anti-estrogen drugs that have no agonistic effects may have benefits in a wide range of cancers, independently of the expression of estrogen receptors in tumor cells, and may synergize with immunotherapies to significantly extend survival.

Keywords

MDSC; tumor immunology; tumor microenvironment

Introduction

Estrogens are pleiotropic steroid hormones known to influence many biological processes that ultimately affect homeostasis, such as development and metabolism. Estrogens bind to two high-affinity receptors (ERs; α and β) that activate similar but not identical response elements and are differentially expressed in multiple tissues. Due to their pathogenic role in accelerated malignant progression, ER^+ breast cancers have been commonly treated with tamoxifen. Tamoxifen, however, has mixed antagonist/agonist effect on on ERs, depending on cell type (1). Correspondingly, alternative interventions are currently evolving as results from clinical testing emerge (2). In contrast to breast cancer, anti-estrogen therapies have proven to be effective in only some ovarian cancer patients (3-7). However, these studies were exclusively focused on ER^+ cancer patients, which represent only 31% of ovarian cancer patients for ERα and 60% of patients for ERβ and did not provide any insight into the effects of estrogen activity on non-tumor cells.

Besides tumor cells, the tumor microenvironment plays a critical role in determining malignant progression as well as response to various therapies. In particular, it is becoming evident that tumors elicit immune responses that ultimately impact survival. In ovarian cancer, for instance, the presence of tumor-infiltrating lymphocytes is a major positive prognostic indicator of tumor survival (8), and multiple T-cell inhibitory pathways have been identified (9-11).

In addition to tumor cells, both ERs are expressed by most immune cell types, including T-cells, B-cells and NK cells, in which ERα 46 is the predominant isoform (12). Correspondingly, estrogens influence helper CD4 T cell differentiation favoring humoral Th2 over cell-mediated Th1 responses (13). Pre-menopausal women have higher levels of estrogen than men, which may contribute to differences in the incidence of certain autoimmune diseases. Notably, various cancers exhibit sex biases that are at least partly explained by hormonal differences. Obesity, which is associated with increased adipocyte production of estrogens, is also a risk factor for a number of cancers. Changes in estrogen levels in women caused by menstruation, menopause, and pregnancy are associated with changes in the immune system, which could ultimately affect disease susceptibility. Despite growing evidence implicating estrogen as a fundamental mediator of inflammation, currently little is known about its potential role in antitumor immune responses, and particularly in patients without direct estrogen signaling on tumor cells but with a strongly responsive immune-environment.

Among suppressors of anti-tumor immune responses, factors driving tumor-associated inflammation universally induce aberrant myelopoiesis in solid tumors, which fuels malignant progression in part by generating immunosuppressive myeloid cell populations (14). In ovarian cancer, deregulated myelopoiesis results in the mobilization of myeloid-derived suppressor cells (MDSCs) from the bone marrow (15) and, eventually, the accumulation of tumor-promoting inflammatory Dendritic Cells (DCs) with immunosuppressive activity in solid tumors (16, 17), while canonical macrophages buildup in tumor ascites (16, 18). Although all these cell types express at least ERα and are influenced by estrogen signaling (19-21), how estrogens impact the orchestration and maintenance of protective anti-tumor immunity remains elusive. Here, we show that estrogens, independently of the sensitivity of tumor cells to estrogen signaling, are a crucial mechanism underlying pathological myelopoiesis in ovarian cancer. We report that estrogens drive MDSC mobilization and augment their immunosuppressive activity, which directly facilitates malignant progression. Our data provide mechanistic insight into how augmented estrogenic activity could contribute to tumor initiation (e.g., in BRCA1-mutation carriers (22)), and provide a rationale for blocking estrogen signals to boost the effectiveness of anti-cancer immunotherapies.

Results

Estrogen signaling impairs protective immunity against ovarian cancer independent of tumor cell signaling

Nuclear expression of ERs specifically in neoplastic cells has been identified in human ovarian carcinomas of all histological subtypes, with positive signal in ~60% of high-grade serous tumors (23). ERα is the predominant estrogen receptor in mouse hematopoietic cells (12). To define the expression of ERα in human ovarian cancer-infiltrating leukocytes, we performed immunohistochemical analysis in 54 serous ovarian carcinomas. Supporting previous reports, we found specific nuclear staining in tumor cells in ~35% of tumors (Figure 1A**, left**). In addition, we identified weaker signals in individual cells in the stroma with leukocyte morphology (different from tumor cell nuclei) in ~20% of ovarian tumors, independent of the ERα status of tumor cells (Figure 1A**, center**). We finally identified 2 specimens that showed specific signals restricted to stromal fibroblasts (Figure 1A**, right**). To confirm that hematopoietic cells at tumor beds express ERα, we sorted ($CD45^+$) cells from 7 different dissociated human ovarian tumors. As shown in Figure 1B and Supplemental Figure 1A, both tumor-infiltrating ($CD11b^+$) myeloid cells and ($CD11b^-$) non-myeloid leukocytes express variable levels of ERα. In addition, both myeloid and lymphoid cells sorted from either the bone marrow of a cancer patient or the peripheral blood of 5 ovarian cancer patients were also $ERα^+$ (Figures 1B&C, and Supplemental Figures 1A&B), suggesting that in addition to potentially having tumor cell-intrinsic effects, estrogens may also play wider a role in shaping the tumor immune-environment. To determine the role of estrogen signaling in tumor-promoting inflammation or anti-tumor immunity, we used a preclinical model of aggressive ovarian cancer in which syngeneic epithelial ovarian tumor cells (ID8-*Defb29/Vegf-a*) develop intraperitoneal tumors and ascites that recapitulate the inflammatory microenvironment of human ovarian tumors (9, 15, 17, 24). Importantly, no ERα was detected in these tumor cells, unlike tumor-associated myeloid cells (Figure 1D).

Of note, ID8-*Defb29/Vegf-a* cells fail to respond to E2 (E2) treatment or the ER antagonist fulvestrant *in vitro*, unlike established estrogen-responsive MCF-7 cells (Figure 1E). Supporting a tumor cell-independent role of estrogen signaling in malignant progression, oöphorectomized (estrogen-depleted) wild-type mice survived significantly longer than non-oöphorectomized, aged-matched controls after orthotopic tumor challenge in multiple independent experiments (Figure 1F), while estrogen supplementation further accelerated malignant progression and reversed the protective effects of oöphorectomy (Figure 1F and Supplemental Figure 1C). Strikingly, the survival benefit imparted by oöphorectomy disappeared in tumor-bearing immunodeficient RAG1-deficient KO mice (Figure 1G), indicating that an adaptive immune response is required for the protective effects of estrogen depletion.

Interestingly, *ad libitum* E2 supplementation resulted in augmented T-cell inflammation at tumor (peritoneal) beds (Figure 2A). However, the proportions of antigen experienced ($CD44^+$), recently activated ($CD69^+$) tumor-associated CD4 and CD8 T-cells were significantly higher in oöphorectomized tumor-bearing hosts, with corresponding decreases in E2-supplemented animals (Figure 2B). Accordingly, the frequencies of T cells isolated from the peritoneal cavity of oöphorectomized tumor-bearing mice producing interferon (IFN)-γ in response to cognate tumor antigens were significantly higher than those generated by control (non-oöphorectomized) mice in conventional ELISpot analysis (Figure 2C), indicative of superior T cell-dependent anti-tumor immunity in the former. Consistently, tumor-associated T cells from E2-treated mice responded significantly worse than either group (Figure 2C). Taken together, these results demonstrate that human ovarian cancer microenvironmental hematopoietic cells express ERα, and that, independent of a direct effect on tumor cells, estrogens accelerate ovarian cancer progression through a mechanism that blunts protective anti-tumor immunity.

ERα signaling in hematopoietic cells enhances ovarian cancer-induced myelopoietic expansion

The benefits of estrogen depletion were not restricted to ID8-*Defb29/Vegf-a* tumors, because the progression of estrogen-insensitive (Supplemental Figure 1D), intraperitoneal Lewis Lung Carcinomas (LLC) was also significantly delayed in oöphorectomized mice, ultimately resulting in decreased survival (Figure 3A**, left**), while E2 supplementation accelerated flank tumor growth (Figure 3A**, right**). Further supporting the general applicability of this mechanism, E2 supplementation also accelerated the growth of estrogen-insensitive (Supplemental Figure 1E) syngeneic A7C11 mammary tumor cells, derived from autochthonous p53/Kras-dependent mammary tumors (15) (Figure 3B). Finally, E2 treatment also increased the number of lung metastases in a model of I.V. injected (estrogen-insensitive) B16 melanoma cells (Figure 3C and Supplemental Figure 1F).

To determine the mechanism by which estrogen signaling accelerates malignant progression, we next investigated differences in the mobilization of immunosuppressive cells. We identified strong estrogen-dependent differences only in the accumulation of MDSCs, both in the spleen (Figure 3D&E) and at tumor beds (Figure 3F&G), which persisted in tumors of similar size (Supplemental Figure 1G). Hence, estrogen treatment increased the percentage

and total numbers of both Ly6C^{high} Ly6G^{-} myelomonocytic (M-MDSC) and Ly6C^{+} Ly6G^{+} granulocytic MDSCs (G-MDSC) in tumor-bearing mice, while estrogen depletion through oöphorectomy significantly decreased their percentage and total numbers both in the spleen and at tumor beds (Figure 3D-G).

To define whether estrogen-driven MDSC mobilization is sufficient to explain accelerated tumor growth, we depleted MDSCs with anti-Gr1 antibodies in A7C11 breast tumor-bearing mice. As expected, oöphorectomized mice injected with an irrelevant IgG again showed accelerated tumor progression when E2 was supplemented *ad libitum* throughout disease progression (Figure 3H). However, differences in tumor growth were completely abrogated when MDSCs were depleted with anti-Gr1 antibodies (Figure 3H).

Estrogens primarily signal through the nuclear receptors ERα and ERβ, the former being expressed in virtually all murine hematopoietic cells (20). Further supporting that differences in the ovarian cancer immuno-environment are independent of estrogen signaling on tumor cells, we identified ERα expression in MDSCs derived from tumor-bearing mice (Figure 1D). Importantly, myeloid cells sorted from tumor-bearing mice were also highly effective at suppressing T-cell proliferative responses and therefore are true immunosuppressive MDSCs and not merely immature myeloid cells (Figure 3I and Supplemental Figure 2A), supporting their role in estrogen-dependent abrogation of anti-tumor immunity. Interestingly, G-MDSCs from E2-depleted (oöphorectomized) mice exhibit weaker immunosuppressive potential compared to vehicle or E2-treated mice.

To confirm that ERα signaling is sufficient to mediate accelerated malignant progression, we then challenged ERα$^{-/-}$ and wild-type control mice with orthotopic ID8-*Defb29/Vegf-a* tumors. As shown in Figure 4A, E2 supplementation failed to accelerate tumor progression in ERα KO hosts but again had significant effects in wild-type controls, indicative that estrogen's tumor-promoting responses are attributable to ERα signaling. In addition, accelerated tumor growth depends on ERα signaling specifically on hematopoietic cells because in response to E2 treatment, tumors progress significantly faster in lethally irradiated mice reconstituted with wild-type bone marrow, compared to identically treated mice reconstituted with ERα-deficient bone marrow (Figure 4B). Together, these results indicate that ERα signaling on hematopoietic cells accelerates malignant progression independently of the stimulation of neoplastic cells, through a mechanism that results in the mobilization of (ERα^{+}) immunosuppressive MDSCs.

Estrogens signal through ERα on human and mouse myeloid progenitors to boost the proliferation of regulatory myeloid cells and enhance their immunosuppressive activity

To rule out that estrogen-dependent myeloid expansion in tumor-bearing mice was the result of subtle differences in tumor burden or inflammation, we reconstituted lethally irradiated mice with a 1:1 mixture of CD45.2^{+} ERα$^{-/-}$ and (congenic) CD45.1^{+} ERα^{+} bone marrow and challenged them with orthotopic ovarian tumors. As shown in Figure 4C&D, a significantly higher percentage (3.6-fold) of total (CD11b^{+} Gr-1^{+}) MDSCs arose from ERα^{+} hematopoietic progenitors, compared to ERα-deficient cells. Because reconstitution of total hematopoietic cells occurred at a similar ratio (Figure 4C) and MDSCs mobilization took place in the same host under an identical milieu, dissimilar ERα-dependent MDSC

accumulation can only be attributed to cell-intrinsic ERα^{+} signaling on myeloid precursors (Figure 4E).

To understand how estrogen signaling promotes MDSC expansion, we next differentiated MDSCs *in vitro* by treating naïve wild-type (ERα^{+}) BM with GM-CSF and IL-6. As reported (25), these inflammatory cytokines induced the generation of immature myeloid cells that express Ly6G and Ly6C similar to MDSCs seen *in vivo* (Figure 5A **left**).

Normal cell culture medium drives estrogen signaling due to the presence of various estrogens in FBS (26) in addition to the estrogenic properties of phenol red. Blocking the estrogen activity of cell culture medium with MPP, a selective antagonist of ERα, severely inhibited the expansion of both M-MDSCs and G-MDSCs (Figure 5A**, left &** Figure 5B), similar to *in vivo* in tumor-bearing mice (Figure 4E) and, to an even greater extent, bone marrow-MDSCs expanded with ID8-*Defb29/Vegf-a*-tumor conditioned medium (Supplemental Figure 2B). In addition, the presence ERα antagonists allowed spontaneous differentiation of more mature CD11c^{+} MHC-II^{+} myelomonocytic cells (Figure 5A**, right**). Corresponding to *in vivo* observations (Figure 3F), further addition of E2 resulted in G-MDSCs that were more potently immunosuppressive while abrogation of ERα signaling prevented the acquisition of stronger immunosuppressive activity by G-MDSCs (Figure 5C**, top**). In contrast, E2 did not affect the inhibitory activity of M-MDSCs (Figure 5C**, bottom**) suggesting that the role of estrogens in the accumulation of M-MDSCs is primarily to drive their expansion, although the low yields of BM-MDSCs obtained in the presence of estrogen antagonists precludes testing their suppressive activity.

To support the relevance of ERα signaling in boosting pathological expansion of MDSCs, we finally procured bone marrow from 5 different lung cancer patients, and expanded myeloid cells with GM-CSF and IL-6 (25), in the presence of different concentrations of the ERα-selective antagonist MPP. As shown in Figure 5D, this system results in reproducible expansion of CD11b^{+} CD33^{+} CD15^{+} CD14^{-} MHC-II^{-} granulocytes and CD11b^{+} CD33^{+} CD15$^{-/low}$ CD14^{+} MHC-II^{-} monocytic cells, corresponding to the human counterparts of granulocytic and monocytic MDSCs, along with more mature myeloid cells (Supplemental Figure 2C). Notably, blockade of ERα signaling resulted in a dramatic dose-dependent reduction in the expansion of both MDSC lineages, both at the level of proportions (Figure 5D) and, especially, absolute numbers (Figure 5E). Equally important, analysis of 266 serous ovarian cancer patients in TCGA datasets confirmed that patients with expression levels of the aromatase gene CYP19A1 (the enzyme responsible for a key step in the biosynthesis of estrogens) above the median also exhibit lower expression of CD3e and perforin, indicators of cytotoxic activity and total T cell infiltration, respectively (Figure 5F).

Together, these data show that estrogen signaling through ERα influences myelopoiesis in both mice and humans to boost the expansion of highly immunosuppressive MDSCs in response to inflammatory signals and block their differentiation into MHC-II^{+} myeloid cells. These combined functions of ERα signaling in myeloid cells promote malignant progression through MDSC-mediated immune-suppression.

Estrogen signaling enhances pSTAT3 activity through transcriptional up-regulation of Janus kinase 2 (JAK2) and increased total STAT3 expression in myeloid progenitors

To determine the mechanism by which estrogen signaling promotes MDSC mobilization, we focused on the effect of estrogen signaling on STAT3 signaling, which plays a major role in regulating myeloid lineage cells and MDSC expansion (14). As shown in Figure 6A, levels of $pSTAT3^{Y705}$ were significantly increased in both monocytic and granulocytic MDSCs immunopurified from the peritoneal cavity of oöphorectomized ovarian cancer-bearing mice supplemented with E2, compared to control oöphorectomized mice receiving vehicle. Accordingly, anti-estrogen treatment of *in vitro* BM-MDSC cultures also inhibited STAT3 signaling resulting in lower phospho-STAT3 in both M-MDSCs and G-MDSCs (Figure 6B), confirming that pSTAT3 signaling is enhanced by estrogen activity.

Because STAT3 activation is triggered by IL-6, which was used for *in vitro* MDSC expansion, we next investigated the role of estrogen signaling on IL6R. Treating BM-MDSCs with E2 or anti-estrogens did not elicit changes in surface expression of the IL6Rα chain (Figure 6C**, left**), while gp130 was paradoxically up-regulated by MPP (Figure 6C**, right**). We therefore focused on downstream JAK and SRC kinases, both of which mediate STAT3 phosphorylation, subsequent dimerization, and nuclear translocation following cytokine receptor engagement (27, 28). As shown in Figure 6D, E2 supplementation induced transcriptional up-regulation of Jak2 in cytokine-induced bone marrow MDSCs of both lineages, while no detectable expression or changes were identified for other Jak members (not shown). Accordingly, E2 also induced a reproducible Jak2 up-regulation at the protein level, including higher levels of active (phosphorylated) Jak2 after a short pulse (Figure 6E&F). Notably, estrogen antagonists also reduced the levels of (active) phospho-Src in both M-MDSCs and G-MDSCs, while E2 supplementation also increased Src activity in the former (Figure 6G).

To define which kinase (Jak2 *versus* Src) plays a predominant role in estrogen-dependent MDSC expansion, we expanded BM-MDSCs in the presence of specific Src (Dasatinib), Jak1/2 (Ruxolitinib), or ERα (MPP) inhibitors. As shown in Figure 6H&I, Jak1/2 inhibition had a dramatic negative effect in the differentiation of M-MDSCs. G-MDSC expansion was also heavily decreased upon Jak1/2 inhibition, but concurrent use of ERα antagonists significantly potentiated these suppressive effects (Figure 6H&I). On the other hand, Src inhibition had no effect on preventing G-MDSC differentiation, but resulted in a significant decrease in M-MDSC mobilization, which was further enhanced by additional ERα inhibition (Figure 6I&J). Therefore, concomitant inhibition of ERα signaling and STAT3-activating kinases has stronger negative effects on the expansion of both monocytic and granulocytic MDSC mobilization than inhibition of either pathway individually. Taken together, these data indicate that ERα signaling on myeloid precursors promotes MDSC expansion by driving STAT3 phosphorylation. In M-MDSCs, this occurs through both enhanced (phosphorylated) Src activity and the necessary function of Jak2, while only Jak2 activity is relevant in G-MDSCs.

Taken together, these data indicate that ERα signaling on myeloid precursors promotes MDSC expansion both through driving STAT3 phosphorylation and through a STAT3

independent mechanism. In M-MDSCs, this occurs through both enhanced (phosphorylated) Src activity and the necessary function of Jak2, while only Jak2 activity is relevant in G-MDSCs.

Estrogen also affects other components of the tumor immune-environment

Finally, to rule out that differences in malignant progression due to the direct effect of estrogens on effector T cells, we performed mixed BM chimera experiments in which mice received a 1:1 mixture of ERα$^{-/-}$ and congenic wild-type BM. Compared to ERα$^{-/-}$ T cells, E2-responsive wild-type CD4 and CD8 T cells display a less activated phenotype characterized by lower expression of CD44 (Figure 7A). Correspondingly, the frequencies of wild-type T cells responding to tumor antigens in IFNγ ELISpot re-challenge assays were lower than those of their counterpart ERα$^{-/-}$ T cells, sorted from the same microenvironment (Figure 7B).

To determine the relative importance of these differences in direct ERα signaling in T cells, independent of estrogen-dependent MDSC activity, wild-type and ERα$^{-/-}$ T cells plenocytes were identically enriched for tumor-reactive populations by *ex vivo* priming against tumor lysate-pulsed BMDCs (29, 30), and then adoptively transferred into ovarian cancer-bearing mice. Confirming previous reports (29, 30), both wild-type and ERα$^{-/-}$ T cells significantly extended survival. However, there was no difference between wild-type and ERα KO T cells regardless of whether mice were treated with E2 (Figure 7C). Therefore, while E2 has measurable T cell-intrinsic effects, these are not sufficient to drive differences in malignant progression, and, therefore, E2 effects on immunosuppressive cells, namely MDSCs, are the main driver underlying estrogen-driven tumor acceleration.

Discussion

Here we show that ERα signaling on myeloid precursors is a major contributor to pathological myelopoiesis in cancer, resulting in MDSC expansion and augmented immunosuppressive activity. Accordingly, oöphorectomized mice exhibit delayed malignant progression upon challenge with different estrogen insensitive tumor models, while E2 supplementation has the opposite effects. Supporting the crucial role of spontaneous anti-tumor immunity in this mechanism, differences in tumor growth disappear in T-cell-deficient mice.

Although the role of estrogen signaling in the progression of breast tumors and a subset of ovarian cancer patients has been underscored by the clinical use of ER antagonists, our results demonstrate that estrogens have a profound effect on anti-tumor immunity and tumor-promoting inflammation, independent of their direct activity on tumor cells. Our data therefore provide novel mechanistic insight into how enhanced estrogenic activity contributes to malignant progression in established tumors. Furthermore, our data support that novel anti-estrogen drugs that, unlike tamoxifen (1), have no agonistic effects on non-breast cell types, may have benefits in a wide range of cancers in pre-menopausal women, independently of the expression of ERs in tumor cells. Therefore, anti-estrogens, especially when used as an adjuvant therapy, could synergize with immunotherapies such as checkpoint inhibitors to extend survival significantly. Thus, while bilateral oöphorectomy is standard in

ovarian cancer treatment, our data suggest that ER$^-$ breast tumors and other malignancies in at least pre-menopausal female cancer patients could be delayed by specifically blocking ERα in a systemic manner, especially if complementary immunotherapies are implemented as adjuvant therapy.

Our results also have implications to understand gender-dependent differences in tumor initiation and malignant progression in different malignancies. For example, we showed that responses to αPD-L1 immunotherapy was sex-dependent in hormone-independent melanoma (31). This could be particularly relevant in BRCA1-mutation carriers, where augmented estrogenic signals has been recently demonstrated (22, 32). Furthermore, ERα expression is regulated by BRCA1-dependent ubiquitination (33), so that cancer-predisposing heterozygous BRCA1 mutations could result in increased ER expression, and therefore increase estrogen activity. Whether mobilization of MDSCs in the context of additional inflammatory signals contributes to tumor initiation in BRCA1 mutation carriers demands further experimental proof, but our study suggests this as a likely pathogenic mechanism.

This study contributes to the understanding of the complexity of factors deregulating myelopoiesis (and therefore antigen presentation) in virtually all solid tumor-bearing hosts. Our data indicate that ERα signaling has a triple effect on myeloid bone marrow progenitors by altering pSTAT3 signaling, which drives both expansion and increased survival in these cells (14): on the one hand, estrogens up-regulate JAK2, which mediates STAT3 phosphorylation, as well as total STAT3 itself. Therefore, estrogenic activity prepares the bone marrow for acute expansion of myeloid precursors, but estrogen-dependent mobilization of MDSCs only occurs in the presence of direct inflammatory signals that activate JAK kinases, which may not necessarily be present during the high estrogen phase of the menstrual cycle. These mechanisms appear to be important during pregnancy though, where E2 also drives the expansion and activation of MDSCs (21), but our study demonstrates their relevance in the pathogenesis of women's malignancies.

In summary, our study unveils the role of estrogen signaling in pathological myelopoiesis, and supports that more specific anti-estrogen drugs could complement emerging immunotherapies to significantly extend the survival of cancer patients, independently of the expression of ERs in tumor cells.

Methods

Mice and cell lines

Female 5-8 week old wild-type (WT) C57BL/6 and congenic Ly5.1 mice were purchased from the Charles River Frederick facility. Esr1 knockout (ERα KO) were purchased from The Jackson Laboratory. Oöphorectomies were performed by Charles River staff at 5 weeks of age. Mice were treated with vehicle (0.1% ethanol) or 10 μM E2 (USP grade, Sigma) in drinking water refreshed every 3-4 days. All mice were maintained in specific pathogen-free barrier facilities. All experiments were conducted according to the approval of the Wistar Institute Institutional Animal Care and Use Committee.

ID8 cells were provided by K. Roby (Department of Anatomy and Cell Biology, University of Kansas; in 2011) (34) and retrovirally transduced to express *Defb29* and *Vegf-a* (24). Clones were passaged less than 4 times. MCF-7, B16.F10 and LLC1 cells were obtained from American Type Culture Collection in 2009, 2013 and 2009, respectively, and passaged less than 4 times. Cell lines used in this article were not authenticated by us.

Peritoneal tumors were initiated in mice by injecting 3×10^6 ID8-*Defb29/Vegf-a* cells intraperitoneal (i.p.). Intraperitoneal cells were harvested from tumor-bearing mice by flushing the peritoneal cavity with PBS. Cells were maintained in vitro at 37° C, 5% CO2 by culturing in RPMI+10% FBS or steroid free medium (SFR10), which was comprised of phenol red-free RPMI+ 10% charcoal-stripped FBS. Cells were treated *in vitro* with vehicle (0.1% DMSO) or varying concentrations of E2, fulvestrant, or methylpiperidino pyrazole (MPP) purchased from Cayman Chemical. Cell line proliferation was determined by MTS assay (Promega), and increased/decreased proliferation relative to vehicle was calculated.

The A7C11 mammary tumor cell line was generated by passaging sorted tumor cells from a mechanically disassociated p53/Kras mammary tumor (35). Flank tumors were initiated by injecting 2×10^4 cells into the axillary flank. Tumor volume was calculated as: $0.5 \times (L \times W^2)$, where L is length, and W is width.

For generating mixed BM chimeras, mononuclear BM cells were collected from adult age-matched CD45.1 (congenic) WT or CD45.2 *Esr1*$^{-/-}$ donor mice, and $1–2 \times 10^6$ cells were mixed in a 1:1 ratio and retro-orbitally injected into lethally irradiated (~950 rad) adult recipients. Mixed chimeras were analyzed after 7–8 weeks as indicated.

Human Samples

Human ovarian carcinoma tissues were procured under a protocol approved by the Committee for the Protection of Human Subjects at Dartmouth-Hitchcock Medical Center (#17702) and under a protocol approved by the Institutional Review Board at Christiana Care Health System (#32214) and the Institutional Review Board of The Wistar Institute (#21212263). Bone marrow (BM) was obtained from Stage I-II lung cancer patients scheduled for surgical resection at the Hospital of the University of Pennsylvania and The Philadelphia Veterans Affairs Medical Center with approval from respective Institutional Review Boards. All patients selected for entry into the study met the following criteria: (i) histologically confirmed pulmonary squamous cell carcinoma (SCC) or adenocarcinoma (AC), (ii) no prior chemotherapy or radiation therapy within two years, and (iii) no other active malignancy. BM cell suspension was obtained from rib fragments that were removed from patients as part of their lung cancer surgery. Informed consent was obtained from all subjects.

Flow Cytometry

Flow cytometry was performed by staining cells with Zombie Yellow viability dye, blocking with anti-CD16/32 (2.4 G2), and staining for 30 min at 4°C with the following anti-mouse antibodies: CD45 (30-F11), CD45.1 (A20), CD45.2 (104), CD11c (N418), I-A/I-E (M5/114.15.2), CD3 (145-2C11), Ly6G (1A8), Ly6C (HK1.4), gp130 (4H1B35), IL6R (D7715A7), Gr1 (RB6-4C5) CD4 (RM4-5), CD8b (YTS156.7.7), CD44 (IM7), CD69

(H1.2F3), CD11b (M1/70); or anti-human antibodies: CD45 (HI30), CD11c (Bu15), HLA-DR-APC/Cy7 (L243), CD15 (HI98), CD14 (HCD14), CD11b (ICRF44), CD33 (WM53), CD19 (HIB19). Samples were subsequently run using an LSRII and analyzed using FlowJo.

ELISpot

Dendritic cells (BMDCs) were differentiated by culturing WT mouse bone marrow for 7 days with 20 ng/mL GM-CSF (Peprotech 315-03), added on day 0 and 3, and 10 ng/mL GM-CSF added on day 6. BMDCs were subsequently primed with tumor antigen by pulsing for 24 hours with irradiated (100 Gy+30 minutes UV) ID8-*Defb29/Vegf-a* cells at a ratio of 10:1. ELISPOT assay was performed by stimulating 1×10^5 cells obtained from peritoneal wash with 1×10^4 antigen-primed BMDCs in a 96-well filter plate (Millipore MSIPS4510) coated with IFNγ capture antibody according to manufacturer's guidelines (eBioscience 88-3784-88). Following incubation at 37° C, 5% CO2 for 48 hours, positive spots were developed using Avidin-AP and BCIP-NBT substrate (R&D Systems SEL002).

Adoptive T-Cell Transfer

Naïve T cells were harvested from spleens of WT or ERα KO mice via RBC lysis followed by magnetic bead negative selection to remove non-T cell $B220^+$, $CD16/32^+$, $CD11b^+$ and $MHC\text{-}II^+$ cells and primed for 5 days with BMDCs pulsed with tumor antigen as reported (30). A total of 1×10^6 T cells was injected i.p. 7 and 14 days post tumor injection.

Bone Marrow-Derived MDSC Cultures

Mouse MDSCs were expanded from mouse bone marrow harvested by flushing tibias and femurs with media. Following red blood cell lysis, 2.5×10^6 cells were cultured in 10 mL of RPMI+ 10% FBS augmented with recombinant mouse 40 ng/mL GM-CSF+ 40 ng/mL IL6 (Peprotech) and incubated at 37°C, 5% CO2 3 or 6 days. Vehicle, estradiol, or MPP treatments were added as described above. For 6 day cultures, cytokines and estrogen treatments were refreshed on day 3. Following red blood cell lysis, 2.5×10^6 cells were cultured in 10 mL of RPMI+ 10% FBS augmented with recombinant mouse 40 ng/mL GM-CSF+ 40 ng/mL IL6 (Peprotech) and incubated at 37°C, 5% CO2 3 or 6 days. Vehicle, E2, or MPP treatments were added as described above. For 6 day cultures, cytokines and E2 were refreshed on day 3. Following incubation, floating and adherent cells were collected, and M-MDSCs and G-MDSCs were isolated via Miltenyi MDSC purification kit according to manufacturer's protocol. Human MDSCs were expanded from human lung cancer patient bone marrow acquired as single cell suspensions (see above). Briefly, 2×10^6 cells were cultured in 3 mL of IMDM+ 15% FBS supplemented with recombinant human 40 ng/mL GM-CSF+ 40 ng/mL IL6 (Peprotech) and treated with vehicle, 2μM, or 10μM MPP (see above) for 4 days. Cells were subsequently harvested and analyzed by flow cytometry.

MDSC Suppression Assay

Naïve WT T cells were purified from spleens as described and labeled with the proliferation tracker Cell Trace Violet according to manufacturer protocol. T cell proliferation was stimulated by adding anti-CD3/CD28 mouse T-activator beads (Thermo) at a 1:1 T cell to bead ratio according to manufacturer protocol. T cells (2×10^5) were subsequently co-

cultured with MDSC at 1:4, 1:8, or 1:16 MDSC to T cell ratios and incubated for 3 days prior to flow cytometric analysis.

Western Blot and IHC

Cells were lysed in RIPA buffer supplemented with protease inhibitors, phosphatase inhibitors, and Na3VO4 (Thermo) according to manufacturer protocol. Protein quantification was determined via BCA assay, and protein was run on TGX 4-15% gradient gels. Following transfer, PVDF membranes were blocked with 5% BSA in TBS+ 0.05% Tween-20. The following primary antibodies were added to membranes, as indicated, and incubated overnight: Jak2 (rabbit clone#D2E12), Stat3 (clone#124H6) and pStat3 (Tyr705, rabbit clone#D3A7), from Cell Signaling; and ERα (Thermo, clone#TE111.5D11) and beta-actin (Sigma, clone#AC-15). Following secondary staining with HRP-conjugated anti-mouse or rabbit IgG, membranes were developed using ECL prime (GE Healthcare).

ERα staining was initially performed in frozen sections from 54 ovarian cancer specimens with clone#TE111.5D11 as primary antibody (Thermo), followed by a biotinylated goat anti-mouse and completion of immunohistochemical procedure according to manufacturer instructions (Vector Labs). Positive staining was confirmed in 19 paraffin-embedded ovarian cancer sections using FDA-approved ER tests (DAKO) in the Laboratory of the Diagnostic Immunohistochemistry at the Hospital of the University of Pennsylvania, following the FDA approved manufacture guidelines.

Quantitative Real Time PCR

Cells were lysed in Trizol buffer and RNA was subsequently purified using RNEasy kit (Qiagen). Reverse transcription was carried out using High-Capacity Reverse Transcription kit (Applied Biosystems). SYBR Green PCR Master Mix (Applied Biosystems) was used with an ABI 7500 Fast Sequence Detection Software (Applied Biosystems). The following primer sequences were used (5′→3′): *Stat3* <F: GACTGATGAAGAGCTGGCTGACT, R: GGGTCTGAAGTTGAGATTCTGCT>; *Jak2* <F: GTGTCGCCGGCCAATGTTC, R: CACAGGCGTAATACCACAAGC>; and *Tbp* (mRNA normalization) <F: CACCCCCTTGTACCCTTCAC, R: CAGTTGTCCGTGGCTCTCTT>.

Expression of human ESR1 was quantified with primers: *ESR1* <F: CCACTCAACAGCGTGTCTC, and R: GGCAGATTCCATAGCCATAC>, and normalized with primers: *GAPDH* <F: CCTGCACCACCAACTGCTTA, R: AGTGATGGCATGGACTGTGGT>.

Expression of mouse ERα was determined with primers: *ERα* <F: GTGCAGCACCTTGAAGTCTCT, R: TGTTGTAGAGATGCTCCATGCC>.

Analysis of TCGA data

Aligned Sequence files related to solid ovarian cancer samples including whole exon sequencing and outcome data were downloaded from TCGA data portal (2015). Scores (number of tags in each transcript) were obtained from each sample, normalized with respect

to total tags in the sample as well as total tags in the chromosome, and expressed as FPKM (fragments/Kb of transcript/million mapped reads).

Supplementary Material

Refer to Web version on PubMed Central for supplementary material.

Acknowledgments

We than the Gabrilovich lab at Wistar for outstanding technical insight.

Financial support: This study was supported by grants to Jose R. Conejo-Garcia (R01CA157664, R01CA124515, R01CA178687, The Jayne Koskinas&Ted Giovanis Breast Cancer Research Consortium at Wistar and Ovarian Cancer Research Fund (OCRF) Program Project Development awards); Tyler J. Curiel (R01CA164122, CDMRP CA140355, P3054174, The Owens Foundation, The Skinner Endowment and OCRF Program Project Development award); Evgeniy B. Eruslanov: RO1CA187392. Michael J Allegrezza and Nikolaos Svoronos (T32CA009171); Kyle K Payne (5T32CA009140-39); and Alfredo Perales-Puchalt (Ann Schreiber Mentored Investigator Award (OCRF)). Support for Shared Resources was provided by Cancer Center Support Grant (CCSG) CA010815 (Dario Altieri).

References

1. Gallo MA, Kaufman D. Antagonistic and agonistic effects of tamoxifen: significance in human cancer. Semin Oncol. 1997; 24:S1-71–S1-80.
2. Sini V, Cinieri S, Conte P, De Laurentiis M, Leo AD, Tondini C, et al. Endocrine therapy in post-menopausal women with metastatic breast cancer: From literature and guidelines to clinical practice. Crit Rev Oncol Hematol. 2016; 100:57–68. [PubMed: 26944782]
3. Hasan J, Ton N, Mullamitha S, Clamp A, McNeilly A, Marshall E, et al. Phase II trial of tamoxifen and goserelin in recurrent epithelial ovarian cancer. Br J Cancer. 2005; 93:647–51. [PubMed: 16222310]
4. del Carmen MG, Fuller AF, Matulonis U, Horick NK, Goodman A, Duska LR, et al. Phase II trial of anastrozole in women with asymptomatic mullerian cancer. Gynecol Oncol. 2003; 91:596–602. [PubMed: 14675683]
5. Smyth JF, Gourley C, Walker G, MacKean MJ, Stevenson A, Williams AR, et al. Antiestrogen therapy is active in selected ovarian cancer cases: the use of letrozole in estrogen receptor-positive patients. Clin Cancer Res. 2007; 13:3617–22. [PubMed: 17575226]
6. Argenta PA, Thomas SG, Judson PL, Downs LS Jr, Geller MA, Carson LF, et al. A phase II study of fulvestrant in the treatment of multiply-recurrent epithelial ovarian cancer. Gynecol Oncol. 2009; 113:205–9. [PubMed: 19239974]
7. Bowman A, Gabra H, Langdon SP, Lessells A, Stewart M, Young A, et al. CA125 response is associated with estrogen receptor expression in a phase II trial of letrozole in ovarian cancer: identification of an endocrine-sensitive subgroup. Clin Cancer Res. 2002; 8:2233–9. [PubMed: 12114425]
8. Zhang L, Conejo-Garcia JR, Katsaros D, Gimotty PA, Massobrio M, Regnani G, et al. Intratumoral T cells, recurrence, and survival in epithelial ovarian cancer. N Engl J Med. 2003; 348:203–13. [PubMed: 12529460]
9. Stephen TL, Rutkowski MR, Allegrezza MJ, Perales-Puchalt A, Tesone AJ, Svoronos N, et al. Transforming Growth Factor beta-Mediated Suppression of Antitumor T Cells Requires FoxP1 Transcription Factor Expression. Immunity. 2014; 41:427–39. [PubMed: 25238097]
10. Cubillos-Ruiz JR, Engle X, Scarlett UK, Martinez D, Barber A, Elgueta R, et al. Polyethylenimine-based siRNA nanocomplexes reprogram tumor-associated dendritic cells via TLR5 to elicit therapeutic antitumor immunity. J Clin Invest. 2009; 119:2231–44. [PubMed: 19620771]
11. Cubillos-Ruiz JR, Martinez D, Scarlett UK, Rutkowski MR, Nesbeth YC, Camposeco-Jacobs AL, et al. CD277 is a Negative Co-stimulatory Molecule Universally Expressed by Ovarian Cancer Microenvironmental Cells. Oncotarget. 2010; 1:329–8. [PubMed: 21113407]

12. Pierdominici M, Maselli A, Colasanti T, Giammarioli AM, Delunardo F, Vacirca D, et al. Estrogen receptor profiles in human peripheral blood lymphocytes. Immunol Lett. 2010; 132:79–85. [PubMed: 20542061]
13. Salem ML. Estrogen, a double-edged sword: modulation of TH1- and TH2-mediated inflammations by differential regulation of TH1/TH2 cytokine production. Curr Drug Targets Inflamm Allergy. 2004; 3:97–104. [PubMed: 15032646]
14. Gabrilovich DI, Ostrand-Rosenberg S, Bronte V. Coordinated regulation of myeloid cells by tumours. Nat Rev Immunol. 2012; 12:253–68. [PubMed: 22437938]
15. Rutkowski MR, Stephen TL, Svoronos N, Allegrezza MJ, Tesone AJ, Perales-Puchalt A, et al. Microbially driven TLR5-dependent signaling governs distal malignant progression through tumor-promoting inflammation. Cancer Cell. 2015; 27:27–40. [PubMed: 25533336]
16. Scarlett UK, Rutkowski MR, Rauwerdink AM, Fields J, Escovar-Fadul X, Baird J, et al. Ovarian cancer progression is controlled by phenotypic changes in dendritic cells. J Exp Med. 2012; 209:495–506. [PubMed: 22351930]
17. Tesone AJ, Rutkowski MR, Brencicova E, Svoronos N, Perales-Puchalt A, Stephen TL, et al. Satb1 Overexpression Drives Tumor-Promoting Activities in Cancer-Associated Dendritic Cells. Cell Rep. 2016; 14:1774–86. [PubMed: 26876172]
18. Huarte E, Cubillos-Ruiz JR, Nesbeth YC, Scarlett UK, Martinez DG, Buckanovich RJ, et al. Depletion of dendritic cells delays ovarian cancer progression by boosting antitumor immunity. Cancer Res. 2008; 68:7684–91. [PubMed: 18768667]
19. Kovats S. Estrogen receptors regulate an inflammatory pathway of dendritic cell differentiation: mechanisms and implications for immunity. Horm Behav. 2012; 62:254–62. [PubMed: 22561458]
20. Kovats S. Estrogen receptors regulate innate immune cells and signaling pathways. Cell Immunol. 2015; 294:63–9. [PubMed: 25682174]
21. Pan T, Zhong L, Wu S, Cao Y, Yang Q, Cai Z, et al. 17 beta-Oestradiol enhances the expansion and activation of myeloid-derived suppressor cells via signal transducer and activator of transcription (STAT)-3 signalling in human pregnancy. Clin Exp Immunol. 2016; 185:86–97. [PubMed: 26969967]
22. Widschwendter M, Rosenthal AN, Philpott S, Rizzuto I, Fraser L, Hayward J, et al. The sex hormone system in carriers of BRCA1/2 mutations: a case-control study. Lancet Oncol. 2013; 14:1226–32. [PubMed: 24140203]
23. Sieh W, Kobel M, Longacre TA, Bowtell DD, deFazio A, Goodman MT, et al. Hormone-receptor expression and ovarian cancer survival: an Ovarian Tumor Tissue Analysis consortium study. Lancet Oncol. 2013; 14:853–62. [PubMed: 23845225]
24. Conejo-Garcia JR, Benencia F, Courreges MC, Kang E, Mohamed-Hadley A, Buckanovich RJ, et al. Tumor-infiltrating dendritic cell precursors recruited by a beta-defensin contribute to vasculogenesis under the influence of Vegf-A. Nat Med. 2004; 10:950–8. [PubMed: 15334073]
25. Marigo I, Bosio E, Solito S, Mesa C, Fernandez A, Dolcetti L, et al. Tumor-induced tolerance and immune suppression depend on the C/EBP beta transcription factor. Immunity. 2010; 32:790–802. [PubMed: 20605485]
26. Briand P, Lykkesfeldt AE. Effect of estrogen and antiestrogen on the human breast cancer cell line MCF-7 adapted to growth at low serum concentration. Cancer Res. 1984; 44:1114–9. [PubMed: 6362856]
27. Murray PJ. The JAK-STAT signaling pathway: input and output integration. J Immunol. 2007; 178:2623–9. [PubMed: 17312100]
28. Rebe C, Vegran F, Berger H, Ghiringhelli F. STAT3 activation: A key factor in tumor immunoescape. JAKSTAT. 2013; 2:e23010. [PubMed: 24058791]
29. Nesbeth Y, Scarlett U, Cubillos-Ruiz J, Martinez D, Engle X, Turk MJ, et al. CCL5-mediated endogenous antitumor immunity elicited by adoptively transferred lymphocytes and dendritic cell depletion. Cancer Res. 2009; 69:6331–8. [PubMed: 19602595]
30. Nesbeth YC, Martinez DG, Toraya S, Scarlett UK, Cubillos-Ruiz JR, Rutkowski MR, et al. CD4+ T cells elicit host immune responses to MHC class II- ovarian cancer through CCL5 secretion and CD40-mediated licensing of dendritic cells. J Immunol. 2010; 184:5654–62. [PubMed: 20400704]

31. Lin PY, Sun L, Thibodeaux SR, Ludwig SM, Vadlamudi RK, Hurez VJ, et al. B7-H1-dependent sex-related differences in tumor immunity and immunotherapy responses. J Immunol. 2010; 185:2747–53. [PubMed: 20686128]

32. Hu Y, Ghosh S, Amleh A, Yue W, Lu Y, Katz A, et al. Modulation of aromatase expression by BRCA1: a possible link to tissue-specific tumor suppression. Oncogene. 2005; 24:8343–8. [PubMed: 16170371]

33. Eakin CM, Maccoss MJ, Finney GL, Klevit RE. Estrogen receptor alpha is a putative substrate for the BRCA1 ubiquitin ligase. Proc Natl Acad Sci U S A. 2007; 104:5794–9. [PubMed: 17392432]

34. Roby KF, Taylor CC, Sweetwood JP, Cheng Y, Pace JL, Tawfik O, et al. Development of a syngeneic mouse model for events related to ovarian cancer. Carcinogenesis. 2000; 21:585–91. [PubMed: 10753190]

35. Rutkowski MR, Allegrezza MJ, Svoronos N, Tesone AJ, Stephen TL, Perales-Puchalt A, et al. Initiation of metastatic breast carcinoma by targeting of the ductal epithelium with adenovirus-cre: a novel transgenic mouse model of breast cancer. J Vis Exp. 2014:51171.

Statement Of Significance

Ablating estrogenic activity delays malignant progression independently of the tumor cell responsiveness, owing to a decrease in the mobilization and immunosuppressive activity of MDSCs, which boosts T-cell-dependent anti-tumor immunity. Our results provide a mechanistic rationale to block estrogen signaling with newer antagonists to boost the effectiveness of novel anti-cancer immunotherapies.

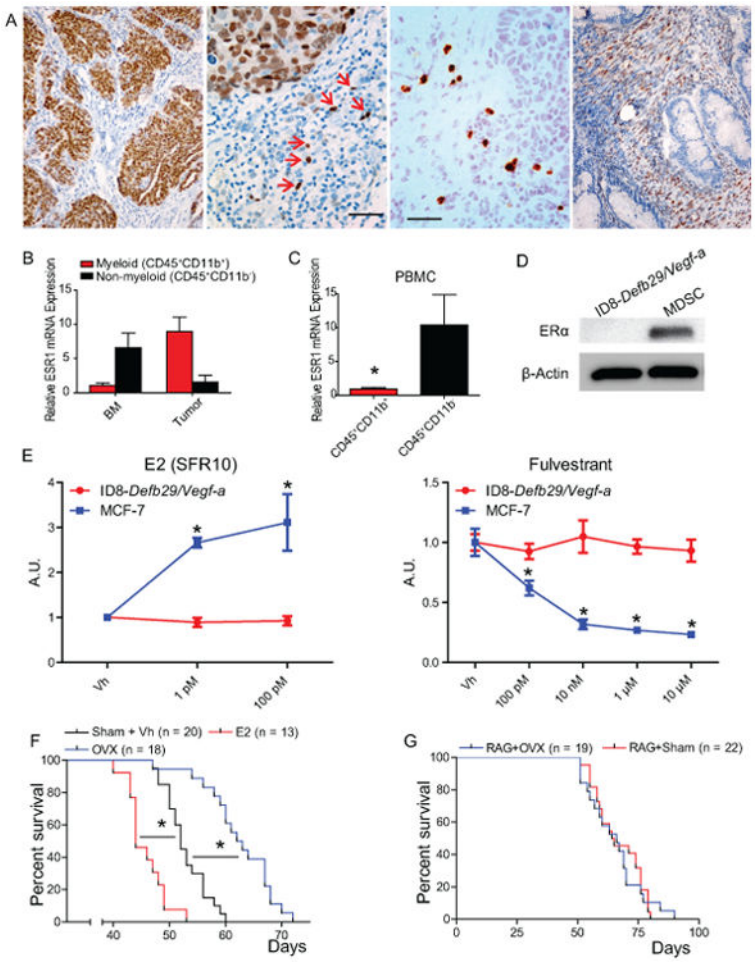

Figure 1. Estrogen-depletion impairment of ovarian tumor progression is independent of tumor cell signaling and is immune dependent

(**A**) Frozen human ovarian tumor sections stained for ERα. Scale bar indicates 1 μm. (**B-C**) Reverse transcription qPCR for *ESR1* expression in myeloid ($CD45^+$ $CD11b^+$) and non-myeloid ($CD45^+$ $CD11b^-$) cells isolated from dissociated ovarian tumor or bone marrow (**B**) or the peripheral blood (**C**) of 5 ovarian cancer patients. (**D**) Western-blot for ERα (66 kDa) expression by ID8-*Defb29/Vegf-a* tumor cells and myeloid-derived suppressor cells isolated from mouse tumors. (**E**) Proliferation relative to vehicle of ID8-*Defb29/Vegf-a* and MCF-7 (positive control) cells in response increasing doses of E2 (in steroid-free media) and the ER antagonist fulvestrant as determined by MTS assay. (**F**) Survival of WT oöphorectomized (OVX) or sham-operated mice challenged with intraperitoneal ID8-*Defb29/Vegf-a* tumors and supplemented or not with E2. Pooled from 3 independent experiments. Total number of mice per group is depicted. (**G**) Survival of OVX or sham-operated *Rag1* KO mice challenged with i.p. ID8-*Defb29/Vegf-a*. pooled from 6 independents Total number of mice per group is depicted. *$p < 0.05$.

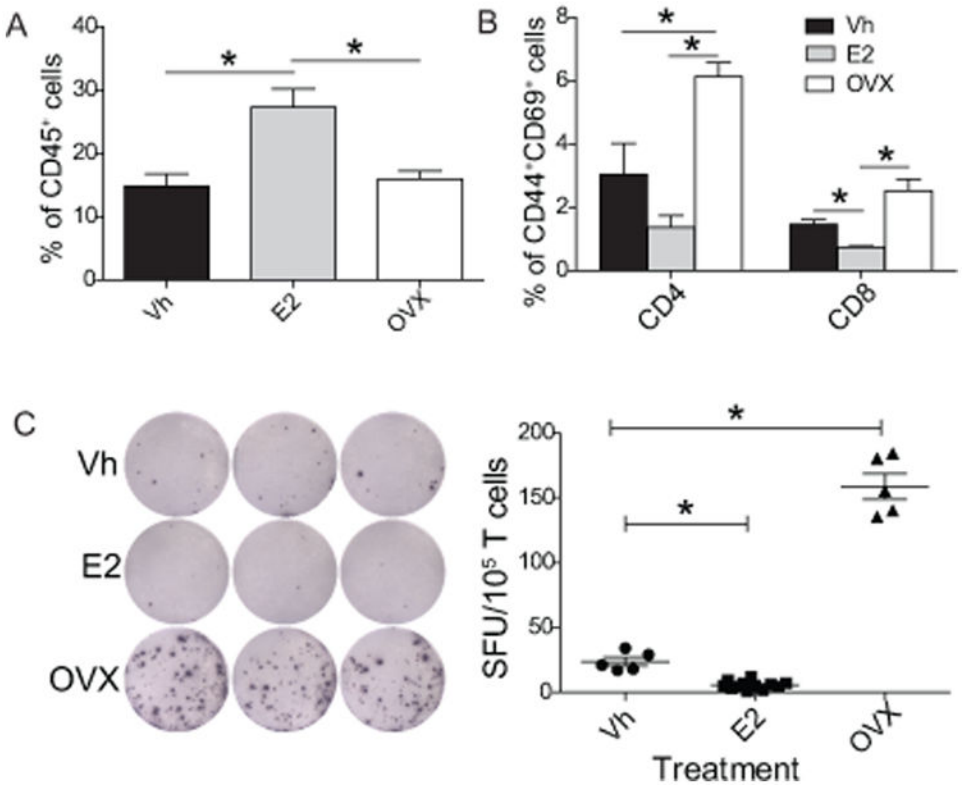

Figure 2. Estrogen suppresses anti-tumor T cell responses

(**A**) Proportion of $CD45^+$ cells isolated from ID8-*Defb29/Vegf-a* peritoneal tumors that are T cells ($CD45^+$ $CD3^+$ γδ-TCR^-). (**B**) Proportion of activated $CD44^+$ $CD69^+$ double positive cells among $CD4^+$ and $CD8^+$ T cells. (**C**) ELISpot analysis of T cells isolated from ID8-*Defb29/Vegf-a* peritoneal tumors stimulated with tumor lysate-pulsed BM-derived dendritic cells. Results shown are representative of multiple independent experiments. *$p < 0.05$.

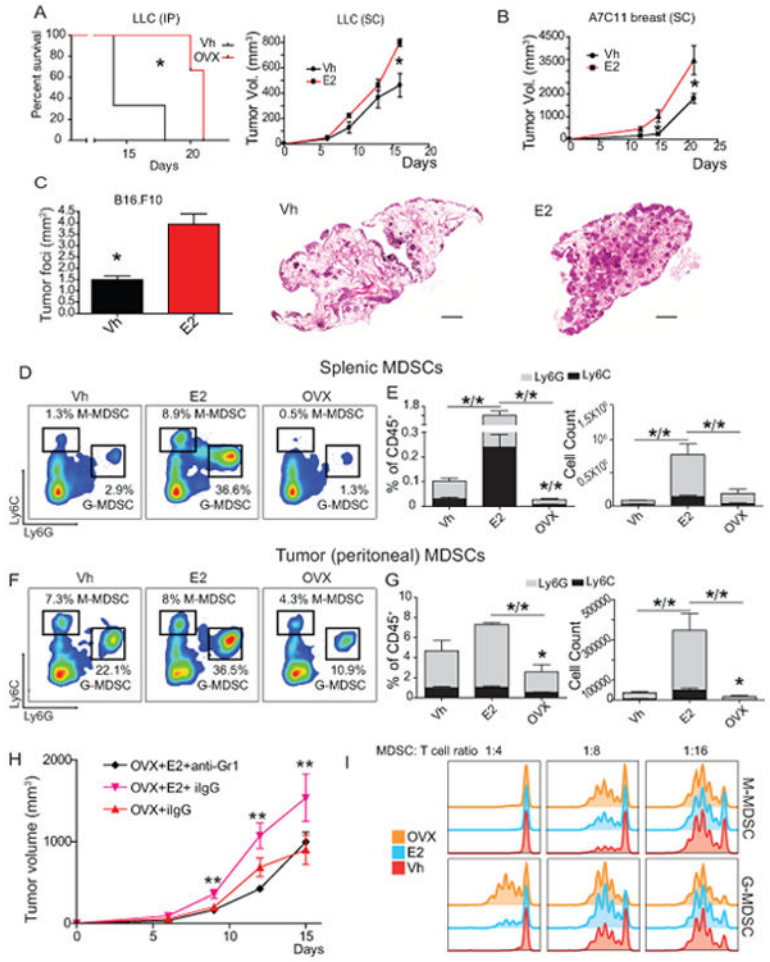

Figure 3. Estrogen drives accumulation of myelomonocytic (M-MDSC) and granulocytic (G-MDSC) myeloid-derived suppressor cells and increases the immunosuppressive potential of G-MDSCs

(**A**) Intraperitoneal LLC lung tumor progression in oöphorectomized *vs.* sham-treated WT mice (**left**) or subcutaneous LLC growth in WT mice treated with vehicle (Vh) *vs.* E2 (**right**) (5 mice/group in both cases). (**B**) Flank A7C11 breast tumor growth in oöphorectomized WT mice treated with vehicle (Vh) *vs.* E2 (5 mice/group). (**C**) 5×10^5 B16.F10 cells (ATCC) were injected I.V. into mice (n=5/group). Upon injection, mice were treated with vehicle (0.1% EtOH) or E2 (10 uM) in drinking water. After 15 days, mice were euthanized and the number of lung metastases per mm^2 was determined by H&E staining. Representative images of lung metastases are also shown. (**D, E**) Expression and quantification of M-MDSCs ($Ly6C^{high}$ $Ly6G^{-}$) and G-MDSCs ($Ly6C^{+}$ $Ly6G^{+}$) in the spleen of ID8-*Defb29/Vegf-a* peritoneal tumor-bearing mice. (**F, G**) Expression and quantification of M-MDSCs ($Ly6C^{high}$ $Ly6G^{-}$) and G-MDSCs ($Ly6C^{+}$ $Ly6G^{+}$) in the peritoneal cavity of ID8-*Defb29/Vegf-a* peritoneal tumor-bearing mice. (**H**) Flank A7C11 breast tumor growth in oöphorectomized mice treated with vehicle (Vh) *vs.* E2 and receiving 250 μg of anti-Gr1 (RB6-8C5; BioXCell) *vs.* control isotype antibodies every other day, starting at day 2 after tumor challenge (5 mice/group). (**I**) Dilution of Cell Trace Violet in labeled T cells activated

with anti-CD3/CD28 beads co-cultured with varying ratios of M- and G-MDSCs isolated from ID8-*Defb29/Vegf-a* tumors. *$p < 0.05$; **$p < 0.01$.

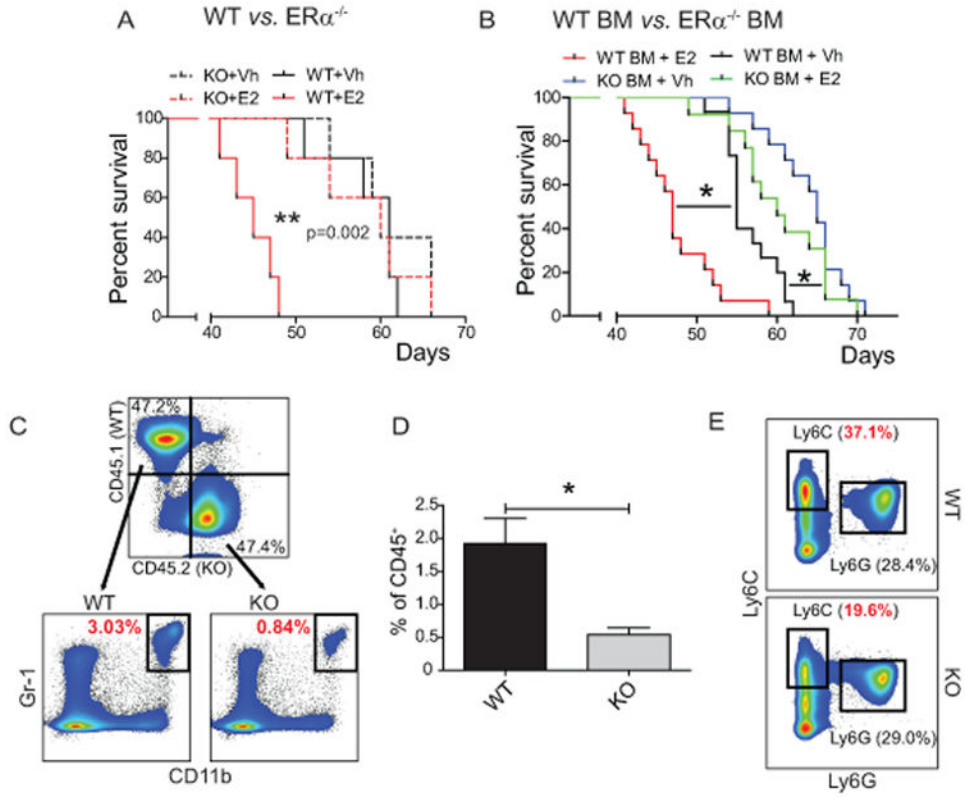

Figure 4. Host estrogen receptor α (ERα) activity is required for E2-driven tumor acceleration and optimal MDSC accumulation

(**A**) Survival of WT and ERα KO mice treated with Vh or E2 and challenged with i.p. ID8-*Defb29/Vegf-a* tumors (n=5 mice/group). (**B**) Survival of WT mice lethally irradiated (10 Gy) and reconstituted with WT or ERα KO bone marrow treated with Vh or E2 and challenged with i.p. ID8-*Defb29/Vegf-a* tumors. Pooled from 3 independent experiments (n≥9 mice/group). (**C**, **D**) Expression and quantification of WT and ERα KO MDSCs ($CD45^+$ $CD11b^+$ $Gr\text{-}1^+$) in the spleens of tumor bearing mice lethally irradiated and reconstituted with a 1:1 mix of WT $CD45.1^+$ and ERα KO $CD45.2^+$ bone marrow. (**E**) Expression of Ly6C and Ly6G by WT and ERα KO $CD11b^+$ $MHC\text{-}II^-$ cells in the spleens of mixed BM reconstituted mice. *$p < 0.05$.

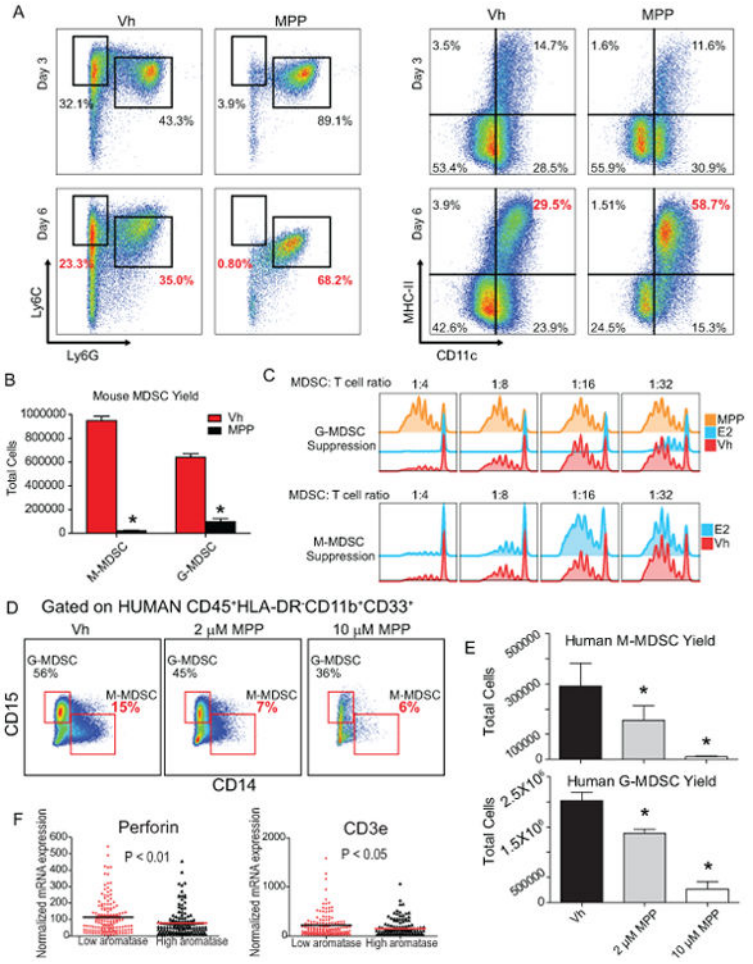

Figure 5. Optimal MDSC expansion and suppressive activity is dependent on estrogen signaling

(**A**) Expression of Ly6C and Ly6G (left) or MHC-II and CD11c (right) by naïve mouse WT bone marrow cultured with GM-CSF+IL6 and treated with Vh or 2 μM anti-estrogen MPP for 3 and 6 days. (**B**) Total number of M-MDSCs and G-MDSCs after culturing naïve WT mouse BM with GM-CSF+IL6 and treating with 2μM MPP for 6 days. Cumulative results of 3 independent experiments. (**C**) Dilution of Cell Trace Violet by labeled T cells activated with anti-CD3/CD28 beads co-cultured with varying ratios of G- or M-MDSCs isolated from 6-day bone marrow cultures treated with Vh, 100 ng/mL E2, or 2 μM MPP. (**D**) Expansion of human M-MDSCs ($CD45^+$ $HLA\text{-}DR^-$ $CD11b^+$ $CD33^+$ $CD14^+$) and G-MDSCs ($CD45^+$ $HLA\text{-}DR^-$ $CD11b^+$ $CD33^+$ $CD15^+$) from lung cancer patient bone marrow cultured in GM-CSF+IL6 and treated with Vh, 2 μM, or 10 μM MPP. (**E**) Total number of human M- and G-MDSCs derived from lung cancer patient bone marrow. *$p < 0.05$. (**F**) Scatter plot of the level of CD3E and PRF1 mRNA (measured as FKPM) in 266 serous ovarian cancers from TCGA datasets, separated by CYP19A1 expression above or below the median.

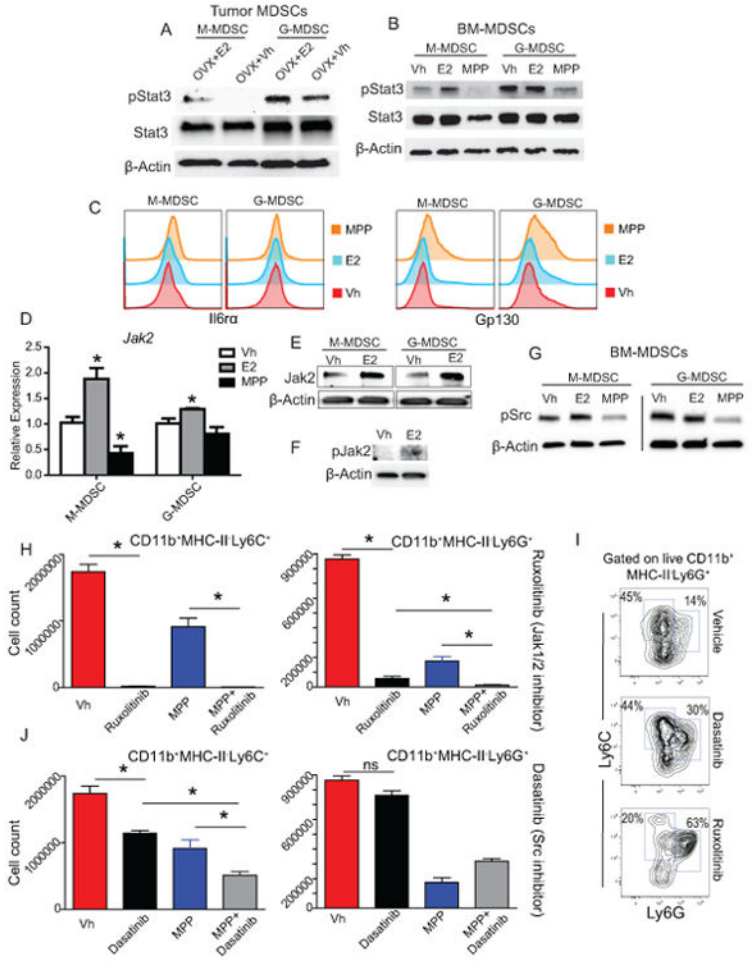

Figure 6. Estrogen increases cytokine-induced STAT3 activation during MDSC expansion

(**A**) Phosphorylated and total STAT3 protein expression in M- and G-MDSCs sorted from the peritoneal cavity of i.p. ID8-*Defb29/Vegf-a* tumor-bearing oöphorectomized mice, supplemented or not with E2 during malignant progression (pooled from 5 animals/group). (**B**) pSTAT3 and total STAT3 protein expression in *in vitro* BM-derived MDSC cultures treated with Vh, 100 ng/mL E2, or 2 μM MPP. (**C**) *In vitro* BM-derived MDSC surface expression of IL6Rα and GP-130 in response to Vh, E2, or MPP treatment. (**D**) *Jak2* RNA expression of *in vitro* BM-derived MDSC in response to estrogen agonists and antagonists. (**E**) Expression of total Jak2 protein under the same conditions. (**F**) Active (phosphorylated) Jak2 protein expression in day 6 *in vitro* BM-derived MDSCs in response to a 5 h. pulse of 100 ng/mL E2. (**G**) pSrc protein expression in *in vitro* BM-derived MDSC cultures treated with Vh, E2, or MPP as in B. (**H**) Live cell counts in day 6. BM-derived MDSC cultures treated with Vh, 2 μM MPP and/or 1μM of Ruxolitinib. Fresh inhibitors were replaced at day 3. (**I**) Ly6C/Ly6G differentiation in BM-MDSC cultures in the presence of Vh, 10 nM of Dasatinib or 1μM of Ruxolitinib. (**J**) Same as in F using Dasatinib instead of Ruxolitinib. *p < 0.05.

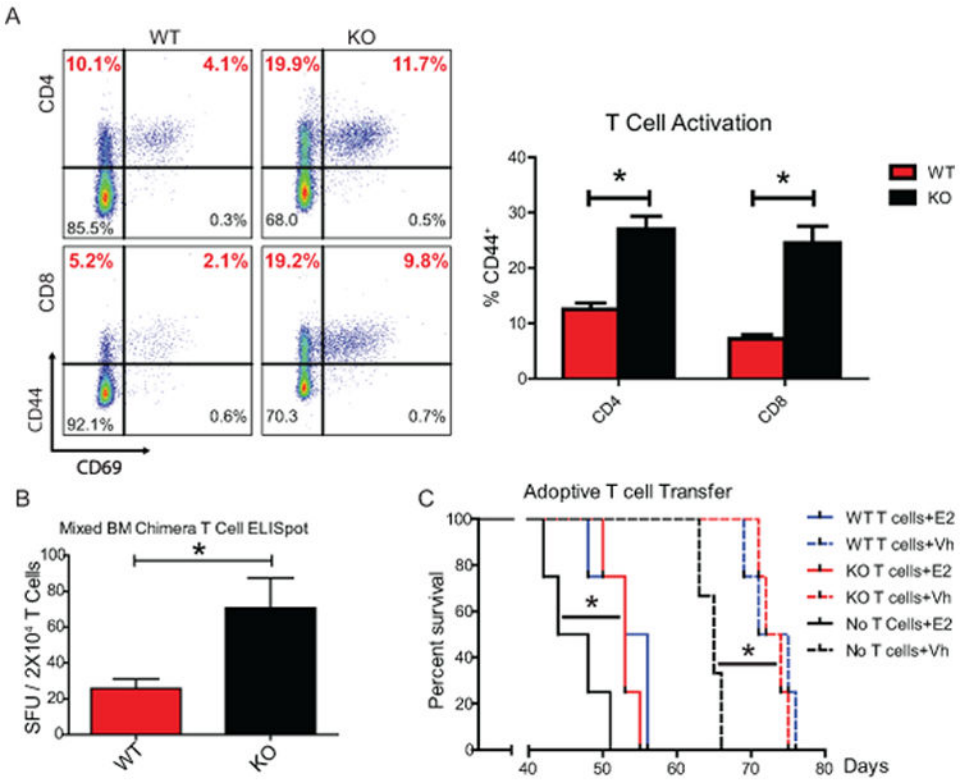

Figure 7. T cell-intrinsic ERα activity suppresses anti-tumor response, but is insufficient to abrogate the effectiveness of tumor-primed T cells

(**A**) Intratumoral T cell expression of CD44 and CD69 in mice lethally irradiated and reconstituted with a 1:1 mix of WT CD45.1$^+$ and ERα KO CD45.2$^+$ bone marrow. (**B**) ELISpot analysis of intratumoral WT and ERα KO T cells FACS-isolated from tumor-bearing mice stimulated with tumor antigen loaded BMDCs. (**C**) Survival of tumor-bearing Vh or E2 treated mice following adoptive transfer of tumor antigen-primed WT or ERα KO T cells. Representative survival curves shown for multiple independent experiments. *$p < 0.05$.